PHYSICAL REVIEW C VOLUME 13, NUMBER 2 FEBRUARY 1976

Features of the (t,p) reaction below the Coulomb barrier of the entrance channel

Y. Iwasaki
Department of Physics, Shizuoka University, Shizuoka, Japan

T. Murata and T. Tamura
NAIG Nuclear Research Laboratory, Kawasaki, Japan

Y. Nogami
Department of Physics, University of Tokyo, Tokyo, Japan
(Received 18 August 1975)

The differential cross sections for the reactions ^{63,65}Cu$(t,p)^{65,67}$Cu were measured at E_t = 3.2, 3.0, and 2.8 MeV. For $L=0$ ground-state transitions, the energy dependence of the values of the differential cross sections is strong and exponential, while the angular distribution shape, which is of a clear diffraction pattern in sharp contrast to the case of the sub-Coulomb (d,p) reaction, does not change with small energy variation. The reactions proceed well below the Coulomb barrier of the entrance channel, yet through a direct process. A definite difference is observed between the angular distributions for the two ground-state transitions. The zero-range distorted-wave Born approximation can reproduce the energy dependence of the differential cross sections and the trend of isotope dependence of the angular distribution. In distorted-wave Born approximation calculations, a definite nuclear optical potential is needed for the triton-nucleus channel which is below the Coulomb barrier, in sharp contrast to the sub-Coulomb (d,p) reaction. The triton-nucleus optical potential below the Coulomb barrier is nearly equal to the optical potential that works at energies of a few tens of MeV. The angular distribution for an $L=2$ transition is forward-rising, though not diffractionlike, and can be reproduced on the whole by the zero-range distorted-wave Born approximation. It is confirmed for the first time that the (t,p) reaction below the Coulomb barrier of the entrance channel takes place in an extended region outside the nucleus. It is argued and concluded on various grounds that the (t,p) angular distribution shape below the Coulomb barrier of the entrance channel is sensitive to the radial two-neutron from factor outside the nucleus. Physical implications of the revealed features are discussed, especially on the coherence of the two-particle form factor and the proton and neutron distributions in the nuclear surface region.

[NUCLEAR REACTIONS ^{63,65}Cu(t,p), $E=2.8$, 3.0, 3.2 MeV; measured $\sigma(E;\theta)$; DWBA analysis. Enriched ^{63}Cu, natural Cu targets, resolution 200 keV; $\theta=10$–165°. Revealed features below the Coulomb barrier, sensitivity to the form factor.]

I. INTRODUCTION

Systematic experiments of the (t,p) reaction were performed first with the tandem accelerator in the Atomic Weapons Research Establishment, Aldermaston, at incident triton energies about 12 MeV,[1,2] and subsequently with the tandem accelerator in Los Alamos Scientific Laboratory at incident triton energies around 20 MeV.[3] The experimental data obtained in the two institutes formed, along with an accumulation of (p,t) reaction data, the basis for extensive theoretical investigations into dynamical aspects of the particle-particle and hole-hole correlations in nuclei.[4–6] Available experimental data of the (t,p) reaction are quite limited, however, in the sense that systematic experiments of the reaction were performed only at two discrete incident energies in only two institutes. The situation is due to poor availability of the radioactive triton beam. It is obviously desirable to have more (t,p) reaction data in wider ranges of energy, in order to achieve more detailed clarification of the interplay of the reaction mechanism and the nuclear structure,[7] and to extract nuclear structure informations more quantitative than ever. Study of the (p,t) reaction cannot be a substitute in general for study of the (t,p) reaction.

In the zero-range distorted-wave Born approximation (DWBA),[4,8] a (t,p) transition from a nucleus with mass number A to a nucleus having mass number $A+2$, with a definite orbital-angular-momentum transfer L and its projection M, is described by the transition matrix element

$$\langle A+2, p|\, V|A, t\rangle_{LM} \propto \int \chi_f^{(-)*}\left(\vec{k}_p, \frac{A}{A+2}\vec{R}\right) Y_{LM}^*(\hat{R}) \times F_L(R)\chi_i^{(+)}(\vec{k}_t, \vec{R}) d^3\vec{R}, \quad (1)$$

where $\chi_i^{(+)}$ and $\chi_f^{(-)}$ are, respectively, the distorted waves in the entrance and exit channels, $\vec{R}$ denotes the radius vector that points to the center of mass of the transferred neutrons from the center of mass of the target nucleus, and $F_L(R)$ is the radial form factor for a (t,p) transition with a definite orbital-angular-momentum transfer L. The form factor $F_L(R)$ is given by

$$F_L(R) = \sum_{\nu_1\nu_2} S(\nu_1\nu_2) F_L^{\nu_1\nu_2}(R) \quad (2)$$

as a coherent sum over a number of pure two-particle configurations $(\nu_1\nu_2)$ with spectroscopic amplitudes $S(\nu_1\nu_2)$, where ν denotes a shell-model single-particle orbit n, l, j.[4,9] Because of the coherence of $F_L(R)$ over various two-particle configurations, the differential cross sections for a (t,p) transition are sensitive, in principle, to the correlations in the wave functions of the nuclear states involved in the transition. However, in practice it has not proved possible to determine the configuration-mixed form factor, i.e., to determine the spectroscopic amplitudes $S(\nu_1\nu_2)$ in (2) by an analysis of experimental data. At best, calculations with some configuration-mixed wave functions that had been deduced from some model or determined by data other than two-neutron-transfer ones were compared with (t,p) or (p,t) experimental data with more or less satisfactory agreements.[10,11] The reason is that, in general, the (t,p) or (p,t) angular distribution shape observed to date is not sensitive to different two-particle configurations for a definite angular-momentum transfer L.[12] At energies where experiments of the (t,p) and (p,t) reactions have been performed, two-neutron transfer takes place in some narrow region around the nuclear surface due to the strong absorption of the triton, and the short wave lengths in both the entrance and exit channels. Therefore the transition matrix element and, in turn, the angular distribution shape turns out to be rather insensitive to the detailed functional form of the radial form factor, being determined essentially by the values of the form factor on the nuclear surface. Furthermore, given a definite value L of the transferred angular momentum, radial form factors for two-particle configurations belonging to one and the same major shell have nearly identical functional forms around the nuclear surface.[4,13] The coherence of the form factor over various two-particle configurations shows up only in the absolute value of the cross section. Consequently, what has been done is to extract some enhancement factors from experimental cross sections[14] in terms of two-particle units calculated on the assumption of some standard wave functions,[4,8] but not to determine the configuration-mixed form factor itself from experimental data. On the other hand, just the insensitivity of the angular distribution shape to the radial form factor provides much reliability to the determination of the angular-momentum transfer L by the experimental angular distribution for a strong transition. In fact, the spin-parity assignment based on the determination of L forms an important result of experimental (t,p) and (p,t) work to date.[2,10,11,14]

At energies below the Coulomb barrier of the triton-nucleus channel there arises a situation that may be called "complementary" to the above-stated one. Namely, the angular distribution shape tends to be sensitive to the radial two-neutron form factor. For the (t,p) reaction, the Coulomb barrier in the entrance channel acts to damp the incident wave inwards, and at the same time stretches extremely its wave length. The region where two-neutron transfer takes place is shifted outwards by the former action of the Coulomb barrier, and is extended by the latter. Indeed, the incident wave is a very slowly varying function of spatial coordinates around the classical distance of closest approach. It decays monotonically from there inwards to the nuclear surface where it begins to suffer strong absorption and distortion by the triton-nucleus optical potential. The product of the distorted wave of the entrance channel decaying inwards with the radial form factor decaying outwards forms a broad hill over a region extending far beyond the nuclear surface. Two-neutron transfer takes place in the region outside the nucleus, and the angular distribution shape turns out to be sensitive to the functional form of the radial form factor in that region. It will be shown in the following that the measurement of the dependence of the angular distribution on the functional form of the radial form factor is feasible with present-day experimental techniques. Physical implications of the fact will be discussed as well.

II. EXPERIMENTAL PROCEDURE

We performed experiments of the reactions ^{63,65}Cu$(t,p)^{65,67}$Cu at the incident triton energies of 3.2, 3.0, and 2.8 MeV.[15] Tritons were accelerated by the Van de Graaff accelerator of the NAIG Nuclear Research Laboratory. Bombarded targets were self-supporting metallic foils of ^{63}Cu isotope and natural Cu with thicknesses of 410 and 250 μg/cm^2, respectively, fabricated by evaporation in

vacuum. The thicknesses were determined by the Rutherford scattering of protons on the targets. The energy losses of 3.0 MeV tritons in the targets are 48 and 29 keV, respectively. The protons from the (t,p) reaction were detected by two silicon semiconductor detectors mounted on two rotatable arms. They were of the Li-drifted type with depletion layers about 2 mm thick. The solid angle subtended by each detector was 3.8×10^{-3} sr. It was defined by an 8.0 mm diam circular aperture in a tantalum plate placed 3 mm before the detector surface. A gold plate with a 6 mm diam circular aperture located 60 mm before the tantalum one served as a baffle to prevent scattering-in of background particles. Elastically scattered tritons as well as deuterons and α particles from the (t,d) and (t,α) reactions were stopped in 40 μm-thick gold absorbers just in front of the detectors. Use of the thick absorbers worsened the over-all energy resolution for protons to about 200 keV. Due care was taken to reduce the background. The Faraday cup as well as the internal surface of the vacuum chamber around the Faraday cup were covered with 0.1 mm tantalum plates, as was the surface of the target holder facing the incident triton beam. Possible variations in the conditions of the target and the beam were monitored by detection of scattered tritons with a silicon surface-barrier detector placed at 165°. Monitoring at a backward angle was effective in checking a very small amount of stray beam which could yield an intolerable amount of background. The diameter of the circular beam spot on the target was about 1 mm.

Successful measurement of very small cross sections below the Coulomb barrier depends critically on overcoming the effects of target contaminants having atomic numbers smaller than that of the target material. Our previous experience showed that silicon was the most prevalent contaminant next to carbon and oxygen. In the present case, contamination by carbon and oxygen poses no problem, because the Q values for the (t,p) reactions on carbon and oxygen are much smaller than those for the ^{63,65}Cu$(t,p)^{65,67}$Cu reactions. On the contrary, the Q value for the (t,p) reaction on silicon is larger than those for the ^{63,65}Cu$(t,p)^{65,67}$Cu reactions. Therefore, it is necessary to suppress contamination by silicon as far as possible. This is achieved effectively, in the present case of metallic copper targets, by fabricating targets by evaporation in vacuum, because the vapor pressure of silicon is smaller than that of copper by three or more orders at suitable temperatures (around or below 1400 K). Data for subtraction of possible contributions of the ^{28}Si-$(t,p)^{30}$Si peaks were obtained with a SiO_2 target.

Spectra for the ^{65}Cu$(t,p)^{67}$Cu reaction were obtained by subtraction of the spectra for the ^{63}Cu target from those for the natural Cu target. This procedure was intentionally adopted in order to determine the ratio between the cross sections for the ground-state transitions in the ^{63}Cu$(t,p)^{65}$Cu and ^{65}Cu$(t,p)^{67}$Cu reactions without any systematic errors in target thickness or beam-detector geometry which could amount to several tens of percent. The advantage of the procedure was partly counteracted by the lower statistics due to using an effectively thinner target for the ^{65}Cu$(t,p)^{67}$Cu reaction. However, the method for statistical evaluation of such experimental data is well known. The ratio between the differential cross sections for the two ground-state transitions is determined independently for each set of angle and incident energy. Therefore, the ratio between the summed or integrated cross sections for the two transitions at an incident energy is determined with an accuracy that is sufficient for the discussions to follow, even if the accuracy for the ratio between the differential cross sections for each angle is not very high.

III. EXPERIMENTAL RESULTS

Typical proton energy spectra are shown in Fig. 1. Small contaminant peaks are observed and assigned to the ^{28}Si$(t,p)^{30}$Si reaction, besides the giant peaks for carbon and oxygen. The contributions of the peaks were subtracted when necessary using the ^{28}Si$(t,p)^{30}$Si spectra measured with a SiO_2 target, to deduce the differential cross sections for the ^{63,65}Cu$(t,p)^{65,67}$Cu reactions. They are less than the statistical errors for the ground-state transitions in the ^{63,65}Cu$(t,p)^{65,67}$Cu reactions for a major fraction of measurements. However, adding to low statistics and bad energy resolution,

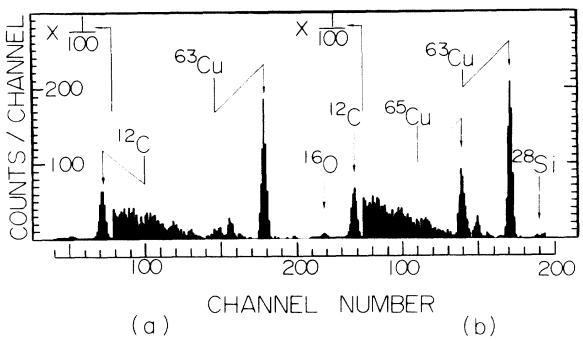

FIG. 1. Proton energy spectrum for the (t,p) reaction on (a) a ^{63}Cu target and (b) a natural Cu target at $E_t=3.2$ MeV, 45° c.m. Each arrow points to the peak corresponding to the ground-state (t,p) transition from the nuclide indicated over it.

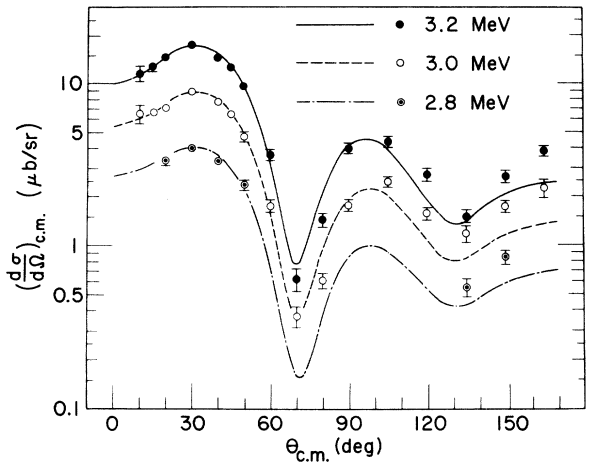

FIG. 2. Differential cross sections for the $L=0$ ground-state transition in the $^{63}Cu(t,p)^{65}Cu$ reaction at $E_t=3.2$, 3.0, and 2.8 MeV. The absolute cross section scale is correct within ±20%. The curves represent results of DWBA calculations. Normalization to the experimental data is made at 30° c.m., $E_t=3.2$ MeV.

they obscure seriously most of the peaks for transitions to excited states. Other contaminants might have been present. In fact, some indication was found for the presence of sulphur. It is estimated that the over-all contributions of contaminants other than silicon do not exceed those of silicon.

Figure 2 shows the differential cross sections for the $L=0$ ground-state transition in the reaction $^{63}Cu(t,p)^{65}Cu$ at $E_t=3.2$, 3.0, and 2.8 MeV. It is readily seen that the reaction takes place well below the Coulomb barrier of the entrance channel as well as through a direct process. The absolute value of the cross section varies exponentially with energy, while the angular distribution shape does not change with small energy variation. It should be noted that the angular distribution shape is of a forward-rising, clear diffraction pattern, in sharp contrast to the case of the well-known sub-Coulomb (d,p) reaction.[16-18] The absolute cross section scale is estimated to be correct within ±20%. Major contributions to the cited error come from uncertainties in the beam-detector geometry. The absolute differential cross sections for the $^{63}Cu(t,p)^{65}Cu$ reaction were measured independently with the ^{63}Cu and natural Cu targets. The results obtained with the two targets were in agreement with each other within statistical errors. Double measurement of the $^{63}Cu(t,p)^{65}Cu$ reaction with different targets was also helpful in estimating the degree of contamination, and greatly increased the reliability of the results.

Figure 3 shows that a difference is observed between the angular distribution shapes for the $^{63}Cu(t,p_0)^{65}Cu$ and $^{65}Cu(t,p_0)^{67}Cu$ transitions at $E_t=3.2$ MeV. The differential cross sections for the $^{65}Cu(t,p_0)^{67}Cu$ transition are definitely larger than those for the $^{63}Cu(t,p_0)^{65}Cu$ at backward angles, while both the transitions are of nearly equal strength at the major peak around 30° c.m..

Differential cross sections at $E_t=3.2$ MeV for the (t,p) transition to the second excited state at $E_x=1.12$ MeV in ^{65}Cu are shown in Fig. 4. The angular distribution, though not clearly diffraction-like, is still forward rising.

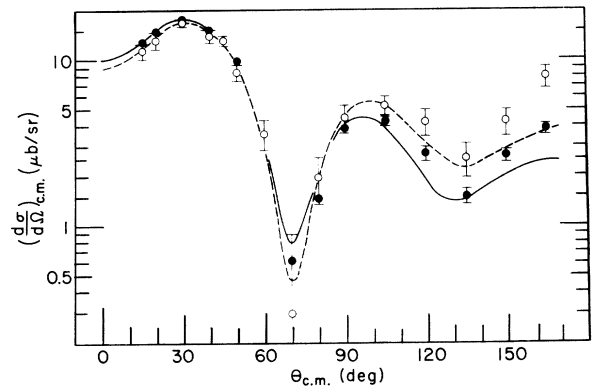

FIG. 3. Differential cross sections for the $L=0$ ground-state transition in the reaction $^{63}Cu(t,p)^{65}Cu$ (full circle, solid line) and for that in the reaction $^{65}Cu(t,p)^{67}Cu$ (open circle, dashed line) at $E_t=3.2$ MeV. Error flags for the $^{63}Cu(t,p_0)^{65}Cu$ transition (see Fig. 2) are omitted in the forward hemisphere for clarity of the figure. The curves represent results of DWBA calculations. Normalization to the data is made at 30° c.m. for each transition.

IV. DWBA CALCULATIONS

The curves drawn in Fig. 2 through Fig. 4 represent results of DWBA calculations[19] made by the

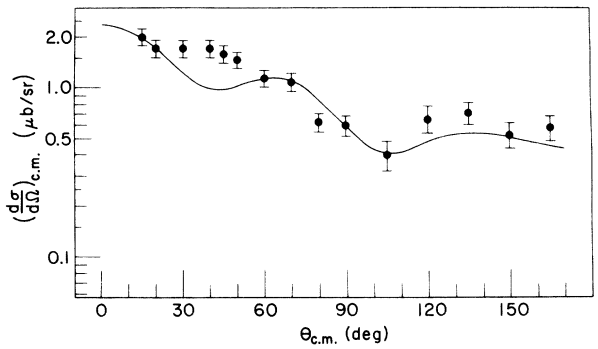

FIG. 4. Differential cross sections for the transition to the second excited state at $E_x=1.12$ MeV in ^{65}Cu in the reaction $^{63}Cu(t,p)^{65}Cu$ at $E_t=3.2$ MeV. The curve represents a result of DWBA calculation, normalized to the data at 15° c.m.

TABLE I. A set of potentials for the incident triton, outgoing proton, and bound neutrons. Notation is the same as in Ref. 24.

	V_S (MeV)	W_S (MeV)	W_D (MeV)	V_{so} (MeV)	r_{0S} (fm)	r_{0I} (fm)	a_S (fm)	a_I (fm)
t	146.0	25.0	0	0	1.24	1.36	0.692	0.890
p	50.7	0	12.5	7.5	1.34	1.34	0.65	0.47
n	Varied [a]	0	0	Varied [b]	1.34	···	0.65	···

[a] See Refs. 4, 9, and 21.
[b] 25 Thomas units.

zero-range DWBA code DWUCK[20] with the set of bound-state and optical potentials shown in Table I. The two-neutron form factor $F_L^{\nu_1\nu_2}(R)$ for a pure two-particle configuration $(\nu_1\nu_2)$ [see Eq. (2)] was calculated by the method of Bayman and Kallio,[21] projecting out the relative-angular-momentum-zero part of the uncorrelated two-particle wave function, with use of single-particle wave functions given by the usual separation-energy prescription.[4,9,21] The curves in Figs. 2 and 3 are for assumed pure $(1f_{5/2})^2$ configuration of transferred neutrons. Normalization to the experimental data is made at 30° c.m., $E_t = 3.2$ MeV for each transition. The DWBA reproduces the angular distribution shape and the energy dependence of the differential cross sections (Fig. 2). It also accounts for the observed trend of the isotope dependence of the angular distribution for the ground-state transition (Fig. 3). These results are stable against small variations of optical potential parameters. The curve in Fig. 4 is discussed in the following section.

The (t,p) reaction below the Coulomb barrier of the entrance channel is in sharp contrast with the well-known sub-Coulomb (d,p) reaction[16-18] in that the (t,p) angular distributions in Figs. 2 and 3 are of a forward-rising, clear diffractionlike pattern. This feature is due to the surface peaking of the (t,p) form factor, strong absorption of the triton, and the large positive Q value of the (t,p) reaction. Because of the large positive Q value, the outgoing proton interacts with the residual nucleus above the Coulomb barrier of the exit channel. This requires in DWBA calculations that a correct nuclear optical potential should be used not only in the exit channel, but also in the entrance channel which is below the Coulomb barrier.[22] If, for example, a purely Coulomb-distorted wave is used for the entrance channel, the calculated angular distribution, as shown in Fig. 5, is neither forward-rising as a whole, nor has peaks and valleys at angles near those observed in the experimental angular distribution (Figs. 2 and 3). A definite nuclear interaction should act to form the distorted wave of the sub-Coulomb triton channel in such a way as to effect proper contributions to the matrix element from inside the nucleus, in sharp contradistinction to the case of the sub-Coulomb (d,p) reaction, where the wave in the exit channel also suffers heavily Coulomb distortion and attenuation.[17] To keep this point clear, we carefully refrain from using the term "sub-Coulomb" (t,p) reaction. Attempting to discover the ranges of triton-optical-potential parameters that can reproduce the experimental angular distributions, we varied the depth V_S of the real central well from 0 to 200 MeV, and the depth W_S of the volume-type imaginary well from 0 to 30 MeV, while the geometrical parameters were fixed at the values obtained at $E_t = 15$ MeV for medium-weight nuclei (family E of Ref. 23). Only two narrow ranges of V_S, i.e., around 145 and 180 MeV, with $W_S > 10$ MeV, were found to be able to reproduce main features of the experimental angular distribution for various proton optical potentials[24,25] employed. Similar ambiguities in the triton-optical-potential parameters at higher energies are reported in the literature.[23,26] The triton optical potential in Table I is not much different from those that work at

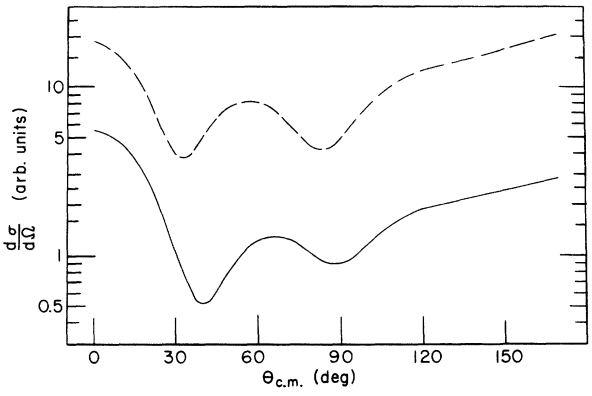

FIG. 5. Angular distributions for the ground-state transition in the reaction $^{63}Cu(t,p)^{65}Cu$ at $E_t = 3.2$ MeV, calculated with pure Coulomb potential in the entrance channel, switching off the nuclear optical potential, for assumed configurations $(1f_{5/2})^2$ (solid line) and $(2p_{1/2})^2$ (dashed line).

energies of a few tens of MeV.[9,23] Thus, the triton optical potential can be extrapolated down to below the Coulomb barrier, its dependence on energy being extremely weak. The high stability of the triton optical potential over a wide energy range is probably due to the presence of a number of exothermic nuclear reactions initiated by the triton. The imaginary part of the triton optical potential seems to be already strong and stabilized at very low energies. Finally, it should be remembered that the usual procedure[23-26] to determine the optical potential by a best fit to elastic scattering data is totally impracticable below the Coulomb barrier. Elastic scattering cross sections deviate from the Rutherford values by not more than a few percent, even at backward angles. Any nuclear optical potential will reproduce elastic scattering cross sections within experimental errors. Goldfarb *et al.* find this difficulty even *near* the Coulomb barrier.[27]

The radius parameters of the real central well and the surface-type imaginary well of the proton optical potential in Table I have the value 1.34 fm, different from the value 1.25 fm in the fixed-geometry Perey potential.[24] Smaller values of the parameters yield calculated angular distributions shifted backwards by as much as 10° compared with the curves in Figs. 2 and 3, and in particular fail to reproduce the major peak around 30° c.m. of the experimental angular distribution, even with variation of other parameters of the proton optical potential over reasonable ranges. It is notable in this concern that the proton optical potential for copper isotopes determined by Perey through a best fit to elastic scattering data at 17 MeV with variation of *all* the parameters, have the values 1.301 and 1.305 fm, respectively, for the radius parameters of the real central well and the surface-type imaginary well.[24] The value 1.34 fm in Table I is not an unreasonable one. Below the Coulomb barrier of the entrance channel, dependences of the calculated angular distribution on the geometrical parameters of the bound-state and optical potentials are more systematically traceable than at higher energies, due to the long wave lengths of both the distorted waves outside the nucleus. Geometrical peculiarities of the DWBA analysis below the Coulomb barrier of the triton-nucleus channel will be reported elsewhere.[28]

V. DISCUSSIONS

A. Sensitivity of the angular distribution shape to the radial two-neutron form factor

There is a clear experimental evidence that the (t,p) reaction below the Coulomb barrier of the entrance channel takes place in an extended region outside the nucleus. We consider the ratio of the intensity of the ^{65}Cu$(t,p_0)^{67}$Cu transition to that of the ^{63}Cu$(t,p_0)^{65}$Cu. At energies sufficiently higher than the Coulomb barrier, it is nearly equal to the square of the corresponding ratio between the form factors at the nuclear surface. The systematic trend of the cross sections for the ground-state (p,t) transitions in the $1f$-$2p$ shell,[9,29-31] as well as available data of the ^{62,64}Ni$(\alpha,p)^{65,67}$Cu reactions[32] indicate that it is smaller than 1.0 by a few tens of percent. On the other hand, the ratio of the summed cross section for the ^{65}Cu$(t,p_0)^{67}$Cu transition to that for the ^{63}Cu$(t,p_0)^{65}$Cu is 1.04 ± 0.04 at $E_t = 3.2$ MeV (Fig. 3). The Coulomb barrier shifts the region important for two-neutron transfer toward larger radii where the ratio of the form factor for the ^{65}Cu$(t,p_0)^{67}$Cu transition to that for the ^{63}Cu$(t,p_0)^{65}$Cu is larger than its value at the nuclear surface. (Fig. 6). This point is corroborated by DWBA calculations, which predict the ratio of the integrated cross section for the ^{65}Cu$(t,p_0)^{67}$Cu transition to that for the ^{63}Cu$(t,p_0)^{65}$Cu to be 1.31, 1.35, and 1.30, respectively, for assumed pure configurations $(2p_{3/2})^2$, $(2p_{1/2})^2$, and $(1f_{5/2})^2$ at $E_t = 3.2$ MeV. The ratio is nearly 1.0 for any pure configuration at sufficiently high energies. It follows, therefore, that the (t,p) transitions at $E_t = 3.2$ MeV proceed dominantly in a region centered around about 7 fm, where the ratio of the form factor for the ^{65}Cu$(t,p_0)^{67}$Cu transition to that for the ^{63}Cu$(t,p_0)^{65}$Cu is larger by 15% or so than its value at the nuclear surface located at about 5 fm (Fig. 6). Rather large absolute values[33] of the cross sections for the ^{63,65}Cu$(t,p_0)^{65,67}$Cu transitions at E_t

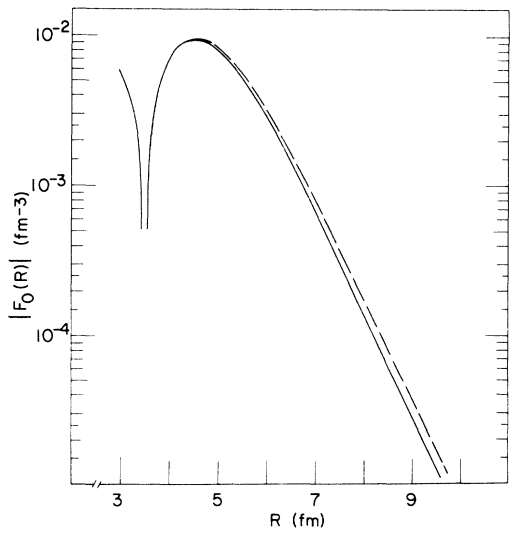

FIG. 6. Form factors for the transitions ^{63}Cu$(t,p_0)^{65}$Cu (solid line) and ^{65}Cu$(t,p_0)^{67}$Cu (dashed line), calculated for the pure configuration $(1f_{5/2})^2$.

= 3.2 MeV indicate that the region where the transitions take place is an extended one. Namely, contributions to the transition matrix elements come from a wide region ranging from the nuclear surface to several femtometers out of the nucleus. Therefore, it is natural that the matrix element, and in turn the angular distribution for the (t,p) reaction, is sensitive to the functional form (logarithmic derivative, to the first approximation) of the form factor in that region.

As shown in Fig. 3, there exists a definite difference between the angular distributions for the ^{63}Cu$(t,p_0)^{65}$Cu and ^{65}Cu$(t,p_0)^{67}$Cu transitions. This amount of isotope dependence of the angular distribution for the $L=0$ ground-state (t,p) or (p,t) transition between spherical nuclei has not been observed at higher energies. The trend of isotope dependence is reproduced by DWBA calculations. This is not peculiar to the two-neutron configuration $(1f_{5/2})^2$ which is assumed for the curves in Fig. 3. The two-neutron configurations $(2p_{1/2})^2$ and $(2p_{3/2})^2$ also reproduce qualitatively the same trend: the differential cross sections for the ^{65}Cu$(t,p_0)^{67}$Cu transition are larger at backward angles and smaller at forward angles than those for the ^{63}Cu$(t,p_0)^{65}$Cu. The difference in angular distribution between the two transitions is brought about by the difference in logarithmic derivative between the corresponding form factors in the region where the (t,p) reaction takes place. The tail of the form factor for the ^{65}Cu$(t,p_0)^{67}$Cu transition falls more slowly than that for the ^{63}Cu$(t,p_0)^{65}$Cu, as shown in Fig. 6, because of the smaller Q value $(7.72\ \text{MeV})^2$ for the former than that for the latter $(9.35\ \text{MeV})^2$.

Figure 7 shows that a sensible difference exists between the angular distributions calculated for the pure configurations $(1f_{5/2})^2$ and $(2p_{1/2})^2$ with one and the same set of potentials (Table I) at E_t = 3.2 MeV for the ^{63}Cu$(t,p_0)^{65}$Cu transition. This feature is very stable against variations of potential parameters. On the other hand, at a sufficiently high energy, the calculated angular distributions for the $(1f_{5/2})^2$ and $(2p_{1/2})^2$ configurations coincide almost perfectly (Fig. 9). It should be

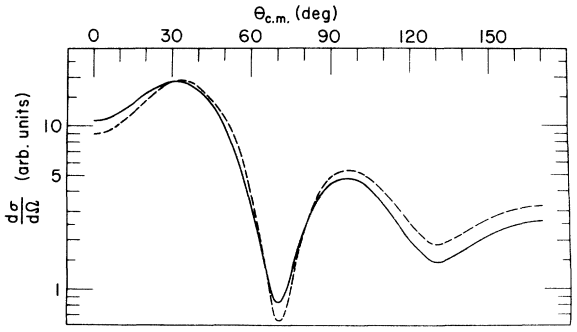

FIG. 7. Angular distributions for the transition ^{63}Cu$(t,p_0)^{65}$Cu at E_t = 3.2 MeV, calculated for the pure configurations $(1f_{5/2})^2$ (solid line) and $(2p_{1/2})^2$ (dashed line).

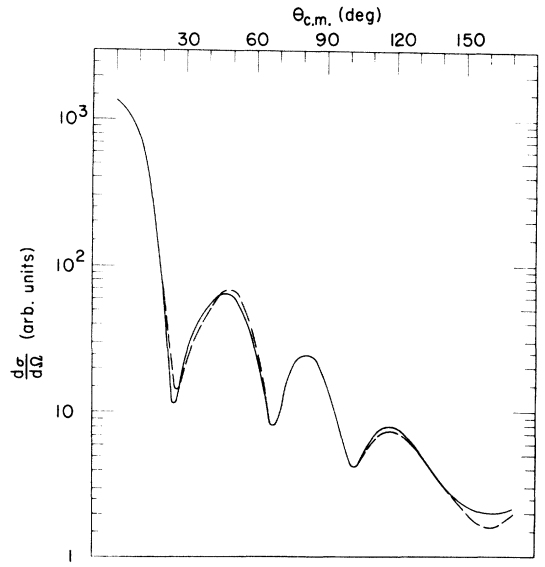

FIG. 8. Angular distributions for the transition ^{63}Cu$(t,p_0)^{65}$Cu at E_t = 12 MeV, calculated for the pure configurations $(1f_{5/2})^2$ (solid line) and $(2p_{1/2})^2$ (dashed line). The curves fit experimental data at E_t = 12 MeV (Ref. 2).

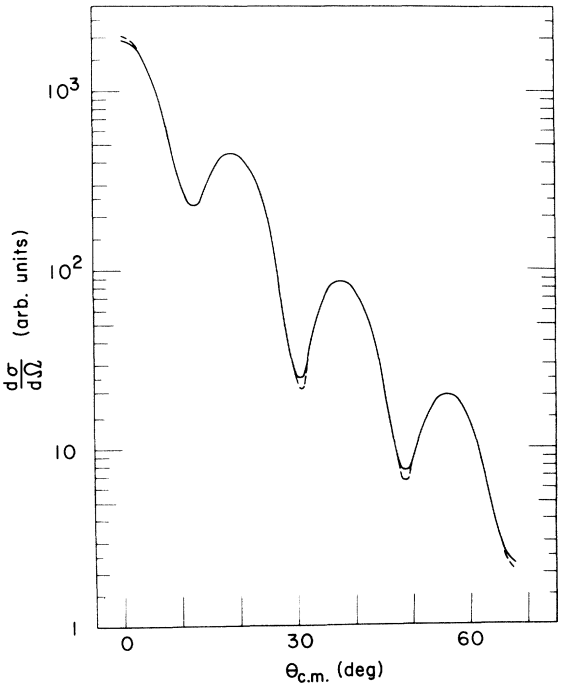

FIG. 9. Angular distributions for the transition ^{63}Cu$(t,p_0)^{65}$Cu at E_t = 43.8 MeV, calculated for the pure configurations $(1f_{5/2})^2$ (solid line) and $(2p_{1/2})^2$ (dashed line). The curves fit experimental data for the inverse transition ^{65}Cu$(p,t_0)^{63}$Cu at E_p = 51.9 MeV (Ref. 31).

appreciated that the configuration dependence of the calculated angular distribution is much amplified as the energy is lowered down to below the Coulomb barrier by comparing Fig. 7 with Figs. 8 and 9. Furthermore, a comparison of Fig. 7 with Fig. 3 reveals that the difference between the solid and dashed curves is of the same character in both the figures. The difference between the calculated angular distributions for the $(1f_{5/2})^2$ and $(2p_{1/2})^2$ configurations is ascribed to the same type of origin as the isotope dependence of angular distribution discussed in the preceding paragraph. In the region important for the (t,p) transition at $E_t = 3.2$ MeV, which extends around 7 fm, as shown above, the logarithmic derivative of the form factor for the $(2p_{1/2})^2$ configuration is smaller in absolute value than that for the $(1f_{5/2})^2$ (Fig. 10), because the angular-momentum barrier for the former is lower than that for the latter; at increasingly larger radii, where the angular-momentum barrier is no longer felt by the bound neutrons, i.e., in the asymptotic region, the two form factors have the same logarithmic derivative determined by the two-neutron separation energy.

Figure 11 compares the calculated angular distributions for the pure configurations $(2p_{1/2})^2$ and $(2p_{3/2})^2$ at $E_t = 3.2$ MeV for the ^{63}Cu$(t,p_0)^{65}$Cu transition. Although the difference in angular distribution shape between the $(2p_{1/2})^2$ and the $(2p_{3/2})^2$ is small, the trend of the difference is quite in parallel with the difference between the $(2p_{1/2})^2$ and

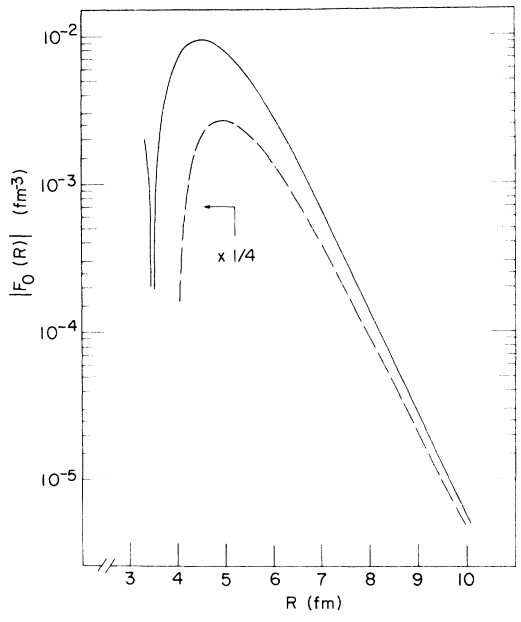

FIG. 10. Form factors for the transition ^{63}Cu$(t,p_0)^{65}$Cu, calculated for the pure configurations $(1f_{5/2})^2$ (solid line) and $(2p_{1/2})^2$ (dashed line).

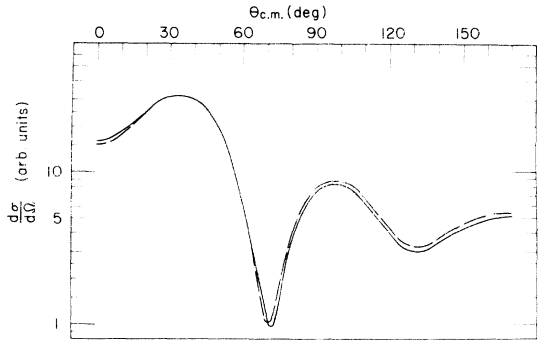

FIG. 11. Angular distributions for the transition ^{63}Cu$(t,p_0)^{65}$Cu at $E_t = 3.2$ MeV, calculated for the pure configurations $(2p_{3/2})^2$ (solid line) and $(2p_{1/2})^2$ (dashed line).

the $(1f_{5/2})^2$ (Fig. 7). The angular-momentum barrier for the bound neutrons is the same for the $(2p_{1/2})^2$ and $(2p_{3/2})^2$ configurations. However, the spin-orbit force, which is repulsive for the $2p_{1/2}$ orbit and attractive for the $2p_{3/2}$, distorts the wave functions of the bound neutrons in such a way as to cause a tighter binding around the nuclear surface region for the $(2p_{3/2})^2$ configuration than for the $(2p_{1/2})^2$. Therefore, the spin-orbit potential makes the logarithmic derivative of the two-neutron form factor smaller in absolute value for the $(2p_{1/2})^2$ configuration than for the $(2p_{3/2})^2$ just outside the nuclear surface. The difference in logarithmic derivative due to the spin-orbit potential, however, is limited to a narrow region adjacent to the nuclear surface, and affects the angular distribution much less than the above-mentioned difference due to the angular-momentum barrier. The spin-orbit potential, as making the wave function in the nuclear surface region larger for parallel spin and orbital angular momenta than for antiparallel ones, is all the same effective in making the absolute value of the two-neutron-transfer cross section larger for a configuration with parallel spin and orbital angular momenta than with antiparallel ones.[9]

The DWBA reproduces the main character of the angular distribution for the (t,p) transition to the second excited state in ^{65}Cu (Fig. 4). However, a substantial discrepancy is observed around 40° c.m.. Further calculational studies are needed to account for it. The second excited state at $E_x = 1.12$ MeV in ^{65}Cu with $J^\pi = 5/2^-$ is interpreted as a particle-vibration-coupled state with a large component of the 2^+ phonon of the core vibration.[34] On the other hand, it is known experimentally that two-neutron transfer at energies higher than the Coulomb barrier excites the 2^+ phonon component of a particle-vibration-coupled state in an odd copper nucleus, and that the odd proton can be consid-

ered a spectator during the reaction process.[31] Therefore, we consider the (t,p) transition to the 1.12 MeV state in ^{65}Cu is with the definite angular-momentum transfer $L=2$, even below the Coulomb barrier of the entrance channel, and calculate the angular distribution for $L=2$. Pure two-neutron configuration $(1f_{5/2})^2$ is assumed. Just as in the case of $L=0$, the calculated angular distribution for an $L=2$ transition is sensitive to the form factor. Figure 12 shows that the slope of the forward-rising angular distribution changes systematically with variation of the binding energy of the transferred neutrons in the final nucleus. Therefore, making a fit to the experimental angular distribution, the binding energy shared by the transferred neutrons can be deduced. The curve in Fig. 4 is calculated with $E_x=1.35$ MeV, which is the excitation energy of the 2^+ phonon state in ^{64}Ni. The agreement between the slopes of the calculated and experimental angular distribution is another evidence of the weak particle-vibration coupling and of the fact that the proton is a spectator to a good approximation.

Summing up the preceding discussions, the (t,p) angular distribution below the Coulomb barrier of the entrance channel depends upon the functional form of the radial form factor outside the nucleus. Together with a reliable method to calculate the two-neutron form factor in a realistic finite well (see below), careful analyses of experimental data having high statistical accuracies will yield valuable informations on the coherence structure of the two-neutron form factor. This type of (t,p) reaction approach to nuclear structure can be systematically exploited in precise comparative studies of the ground and low-lying states in medium-

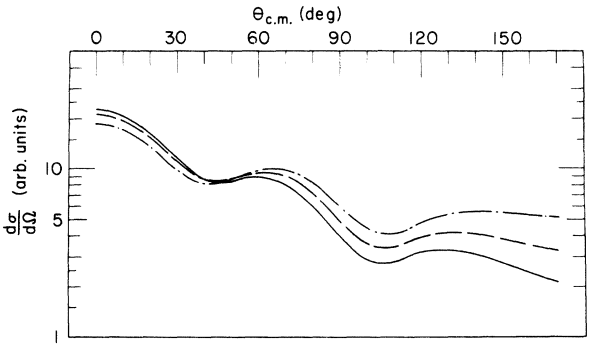

FIG. 12. Calculated angular distributions for an $L=2$ transition in the reaction ^{63}Cu$(t,p)^{65}$Cu at $E_t=3.2$ MeV to an excited state with assumed excitation energies $E_x=0.0$ (solid line), 1.0 (dashed line), and 2.0 MeV (dash-dotted line). Pure $(1f_{5/2})^2$ configuration is assumed. Because of the coupling to the motion of the odd proton which is neglected in the present DWBA formalism, the value of E_x that should be used in calculation is not necessarily equal to the experimental excitation energy.

weight to heavy nuclei with respect to particle-particle correlations. Part of above discussions has been already given in a short note.[35]

Various methods and prescriptions have been presented to calculate the two-neutron form factor.[5,21,9,36-41] Recent developments in finite-well shell-model calculations have been in the direction of extending the functional space by taking into consideration larger and larger numbers of continuum states.[38-41] Apart from some conceptual defects, the main claim against the separation-energy prescription is that it underestimates the absolute cross section.[39-41] Our DWBA calculations reported in the present paper have been performed only with the separation-energy prescription.[9,21] However, our discussion above is certainly safe from possible limitations of the prescription, since the whole discussion is based on relative values of calculated quantities (form factors, differential and integrated cross sections), and since the conclusions are qualitative. Our point is to demonstrate the *experimental* sensitivity of the (t,p) cross section below the Coulomb barrier of the entrance channel to the radial two-neutron form factor in an extended region outside the nucleus, and to indicate the origin of the sensitivity by qualitative arguments and some illustrative calculations. On the other hand, the *experimental* sensitivity below the Coulomb barrier of the entrance channel will serve to discriminate between different *theoretical* form factors, because the region where the latters differ most from each other, in general, lies outside the nucleus.[36-41]

B. Proton and neutron distributions in the nuclear surface region

Possible difference between the proton and neutron distributions in the nuclear surface region is an old[42,43] yet new problem. The (t,p) reaction, together with the isobaric mirror reaction $(^3\text{He},n)$, both below the Coulomb barrier of the entrance channel, can form a new and effective approach to the problem. The same is true for the inverse reactions (p,t) and $(n,^3\text{He})$ below the Coulomb barrier of the exit channels, because it is the ground-state transition that matters in the present context.

On the matter distribution in the nucleus, we have as yet no information of accuracy and reliability comparable to the detailed information[44] on the charge distribution obtained by high-energy electron scattering[45] and muonic isotope shift.[46,47] A large number of physical processes and quantities have been invoked with a view to getting information from them on the difference between the proton and neutron distributions, or in other words between the charge and matter distributions, in the nucleus; (a) elastic scattering of protons at

low energies (tens of MeV),[48] (a′) elastic scattering of nuclear particles heavier than protons,[49] especially heavy ions,[50] (b) Coulomb energy difference between a pair of isobaric analog states,[51] (c) elastic scattering of protons at high energies (GeV region),[52] (d) elastic and charge exchange scattering of pions,[53] (e) high-energy pion-nucleus reaction cross sections,[54] (f) pion production by protons on nuclei,[55] (g) photoproduction of neutral ρ mesons on nuclei,[56] (h) level shift in pionic atoms,[47] (i) the ratio between π^--nucleus and π^+-nucleus reaction cross sections,[43,57,58] (j) absorption of stopped negative kaons,[59,60] (k) absorption of stopped antiprotons.[61] All of the approaches (a) to (h) involve integration over the nuclear volume, and are not particularly sensitive to the structure of the nuclear surface. In general, only one parameter indicating the extent of the nuclear matter distribution, i.e., the half-density radius or root-mean-square radius, can be determined. An overwhelming majority of works show that the matter distribution radius is almost equal with the charge distribution radius.[51,52,54,56-58] On the other hand, (j) and (k) probe directly into the difference between the proton and neutron densities in the nuclear surface region. However, the results obtained to date,[59-61] which indicate much larger probability of finding neutrons than protons in the outermost region of a heavy nucleus, are qualitative from two causes. First, it is practically difficult to attain high statistics. Secondly, fundamental problems of kaon-nucleus and antiproton-nucleus interactions at extremely low energies still remain to be investigated. There is indication that (j) and (k) are processes that take place indeed in the outermost part of the nuclear surface (called by the name of "halo"[60,61]) where the nuclear matter density is very low.[60-62] It is maintained that (i) is sensitive to the difference between the proton and neutron densities in the nuclear surface region.[43,58] However, results of (i)[57,58] are in agreement with most of (b) to (h), and in contradiction to (j) and (k). It is likely that (i) on one hand, and (j) and (k) on the other, probe different parts of the nuclear surface. The present state of affairs is summarized: while the proton and neutron distribution radii are nearly equal, there exists a neutron-rich halo in the tenuous outermost part of a heavy nucleus.[60-62] In spite of a large number of laborious experimental works, there is yet a serious lack of information on the texture of the nuclear surface region.

It is shown in Sec. V A that the differential cross sections for the (t,p) reaction below the Coulomb barrier of the entrance channel are sensitive to the two-neutron form factor outside the nucleus. What is important is that the two-neutron form factor for the ground-state transition is a stable object varying not very fast from neighboring neutron-even to neutron-even nucleus. Furthermore, the matter is certainly the same for the isobaric mirror reaction $(^3\mathrm{He},n)$, although as yet no experimental data are available for the $(^3\mathrm{He},n)$ reaction on medium-weight to heavy nuclei with qualities comparable with those of the (t,p) reaction. The two-particle form factor for $T=1$, $S=0$ can be studied experimentally as a function of radial distance R, and the proton number Z [in the case of $(^3\mathrm{He},n)$] or the neutron number N [in the case of (t,p)].[63] It is experimentally "differentiated" concerning R by varying the incident energy. Also, it is "differentiated" with respect to Z in going from isotone to isotone, or with respect to N in going from isotope to isotope. The value of the form factor at a radial distance off the nuclear surface is very sensitive to the radius and surface-thickness parameters of the nuclear potential that binds the transferred particles. By pursuing the change of the cross section with variation of Z or N, the changes of the radius and surface-thickness parameters over the isotones or isotopes may be deduced. By far the most important, however, is that the difference in proton and neutron distributions in the outermost part of the nuclear surface (the "halo" region) can be directly probed by comparing the $(^3\mathrm{He},n)$ and (t,p) cross sections well below the Coulomb barrier of the entrance channel. Experiments are more feasible and results are likely to be more quantitative than for (j) and (k).

In the point-triton approximation (see Refs. 29, 6), the radial form factor for a pure two-particle configuration is just the product of the two radial single-particle wave functions, apart from a numerical coefficient. In the current zero-range approximation, calculation of the radial form factor involves an integration with respect to the relative coordinates between the two neutrons by which the internal structure of the triton is taken into consideration. Though mediated by an integration, the relation between the radial form factor and the particle density distribution (single-particle wave function) is explicitly well defined. The relation indicates that even the point-triton approximation is reasonable in the region outside the nucleus, where the wave lengths of the distorted waves at low energies are large, and single-particle wave functions are simple and radially monotonous. Configuration mixing introduces only a linear combination over pure two-particle configurations. With just the same extent of analysis as in a conventional nuclear structure problem, the radial form factor can be related to the radial particle density distribution.

VI. CONCLUSIONS

It is confirmed for the first time that the (t,p) reaction below the Coulomb barrier of the entrance channel takes place in an extended region outside the nucleus. A definite nuclear optical potential is required for the triton-nucleus channel which is below the Coulomb barrier, in sharp contrast to the well-known case of sub-Coulomb (d,p) reaction. The triton-nucleus optical potential is nearly independent of energy. The DWBA reproduces the experimental angular distribution, its isotope dependence, and the energy dependence of differential cross sections. The angular distribution shape is sensitive to the functional form of the radial two-neutron form factor outside the nucleus. The (t,p) reaction below the Coulomb barrier of the entrance channel has a number of promising features which warrant systematic experimental studies in the future, in spite of considerable practical difficulties, especially in accelerating particles out of a radioactive gas. It can provide, together with the isobaric mirror reaction $(^3\mathrm{He},n)$, information on the coherence structure of the two-particle form factor for the $T=1$, $S=0$ transfer reactions, the matter distribution in the nuclear surface region, and the difference between the neutron and proton distributions in the outermost "halo" region of the nuclear surface.

ACKNOWLEDGMENTS

The authors are very much indebted to Dr. N. Kawai of the NAIG Nuclear Research Laboratory for making the triton beam available to them. Their deep gratitude is due to Dr. K. Sakurai, Dr. M. Sekiguchi, and Dr. N. Takahashi for contributions in early stages of the experimental work. They are also grateful to Professor H. Ohnuma, Professor T. Suehiro, and a number of colleagues in the Institute for Nuclear Study, University of Tokyo, for interest and support in performing DWBA calculations.

---

[1]R. Middleton and D. J. Pullen, Nucl. Phys. 51, 50, 63, 77 (1964); J. H. Bjerregaard, O. Hansen, O. Nathan, and S. Hinds, *ibid.* 89 , 337 (1966). Further references are found in Ref. 4.

[2]J. H. Bjerregaard, O. Nathan, S. Hinds, and R. Middleton, Nucl. Phys. 85, 593 (1966).

[3]E. R. Flynn, G. J. Igo, R. Woods, P. D. Barnes, and N. K. Glendenning, Phys. Rev. Lett. 19, 798 (1967); E. R. Flynn, J. G. Beery, and A. G. Blair, Nucl. Phys. A154, 225 (1970). Further references are found in Ref. 4. A few works at $E_t = 7.5$ MeV are published, too. For example, D. C. Williams, J. D. Knight, and W. T. Leland, Phys. Rev. 164, 1419 (1967).

[4]R. A. Broglia, O. Hansen, and C. Riedel, in *Advances in Nuclear Physics*, edited by M. Baranger and E. Vogt (Plenum, New York, 1973), Vol. 6, p. 287.

[5]N. K. Glendenning, Phys. Rev. 137, B102 (1965).

[6]S. Yoshida, Nucl. Phys. 33, 685 (1962).

[7]We are aware of a large number of recent works on multistep or channel-coupled processes, although we make no explicit reference to them in the text because of no direct relevance.

[8]R. A. Broglia, C. Riedel, and T. Udagawa, Nucl. Phys. A184, 23 (1972).

[9]B. F. Bayman and N. M. Hintz, Phys. Rev. 172, 1113 (1968).

[10]R. F. Casten and O. Hansen, Nucl. Phys. A210, 489 (1973); E. R. Flynn, J. G. Beery, and A. G. Blair, Nucl. Phys. A218, 285 (1974).

[11]P. T. Debevec and G. T. Garvey, Phys. Rev. C 2, 680 (1974); R. G. Markham and H. W. Fulbright, Nucl. Phys. A203, 244 (1973); D. H. Kong-A-Siou and H. Nann, Phys. Rev. C 11, 1681 (1975).

[12]An exceptional case is found in the paper: R. A. Broglia and C. Riedel, Nucl. Phys. A92, 145 (1967). However, note that the energy is near the Coulomb barrier and the two 0^+ final states discussed in the paper belong to different major shells (see discussions to follow in the text).

[13]R. A. Broglia, C. Riedel, and T. Udagawa, Nucl. Phys. A169, 225 (1971).

[14]H. Orihara, Y. Ishizaki, G. F. Trentelman, M. Kanazawa, K. Abe, and H. Yamaguchi, Phys. Rev. C 9, 266 (1974); J. B. Ball, J. J. Pinajian, J. S. Larsen, and A. C. Rester, *ibid.* 8, 1438 (1973); J. B. Ball, C. B. Fulmer, J. S. Larsen, and G. Sletten, Nucl. Phys. A207, 425 (1973); J. Rapaport, J. B. Ball, and R. L. Auble, *ibid.* A208, 371 (1973); J. S. Larsen, J. B. Ball, and C. B. Fulmer, Phys. Rev. C 7, 751 (1973).

[15]The reactions were studied at $E_t = 12$ MeV (see Ref. 2). However, absolute cross sections are not reported.

[16]E. B. Dally, J. B. Nelson, and W. R. Smith, Phys. Rev. 152, 1072 (1966); M. Sekiguchi, Y. Iwasaki, and K. Sakurai, in Contributions to the International Conference on Nuclear Structure, Tokyo, September 1967 (unpublished), p. 306.

[17]N. Austern, *Direct Nuclear Reaction Theories* (Wiley-Interscience, New York, 1970).

[18]J. Rapaport, A. Sperduto, and M. Salomaa, Nucl. Phys. A197, 337 (1972).

[19]Calculations were performed with the TOSBAC-3400 computer of the Institute for Nuclear Study, University of Tokyo.

[20]P. D. Kunz, University of Colorado (unpublished).

[21]B. F. Bayman and A. Kallio, Phys. Rev. 156, 1121 (1967).

[22]The same situation occurs in the sub-Coulomb (d, n) reaction from a different cause. Namely, the Coulomb barrier is absent in the exit channel from the outset. For example, J. Bommer, B. Efken, H. Fuchs,

K. Grabisch, H. Kluge, W. Ribbe, G. Röschert, and F. Sichelschmidt, Nucl. Phys. A199, 121 (1973). Otherwise see Ref. 17.

[23]J. C. Hafele, E. R. Flynn, and A. G. Blair, Phys. Rev. 155, 1238 (1967).

[24]F. G. Perey, Phys. Rev. 131, 745 (1963).

[25]F. D. Becchetti, Jr., and G. W. Greenlees, Phys. Rev. 182, 1190 (1969).

[26]E. R. Flynn, D. D. Armstrong, J. G. Beery, and A. G. Blair, Phys. Rev. 182, 1113 (1969).

[27]L. J. B. Goldfarb, J. A. Gonzalez, M. Posner, and K. W. Jones, Nucl. Phys. A185, 337 (1972).

[28]Y. Iwasaki (to be published).

[29]G. Bassani, N. M. Hintz, and C. D. Kavaloski, Phys. Rev. 136, B1006 (1964).

[30]N. Auerbach, Phys. Rev. 163, 1203 (1967).

[31]Y. Iwasaki, M. Sekiguchi, F. Soga, and N. Takahashi, Phys. Rev. Lett. 29, 1528 (1972).

[32]D. Bucurescu, M. Ivaşcu, G. Semenescu, and M. Titirici, Nucl. Phys. A189, 577 (1972).

[33]The value of the form factor at 7 fm is one order smaller than the value at the nuclear surface. The amplitude of the incident wave at 7 fm is more than two orders smaller than that at the classical distance of closest approach, which is 14 fm. Therefore, the square of the product of the form factor and the incident wave is attenuated by more than six orders. On the other hand, the observed differential cross sections at $E_t = 3.2$ MeV are smaller than the cross sections for ground-state (t,p) transitions at energies higher than the Coulomb barrier by less than two orders.

[34]A. L. McCarthy and G. M. Crawley, Phys. Rev. 150, 935 (1966).

[35]Y. Iwasaki, T. Murata, T. Tamura, and Y. Nogami, Lett. Nuovo Cimento 12, 586 (1975).

[36]R. M. Drisko and F. Rybicki, Phys. Rev. Lett. 16, 275 (1966).

[37]R. L. Jaffe and W. J. Gerace, Nucl. Phys. A125, 1 (1969).

[38]R. H. Ibarra and B. F. Bayman, Phys. Rev. C 1, 1786 (1970).

[39]R. H. Ibarra, Nucl. Phys. A211, 317 (1973).

[40]F. A. Gareev, J. Bang, and R. M. Jamalejev, Phys. Lett. 49B, 239 (1974).

[41]R. H. Ibarra, M. Vallieres, and D. H. Feng, Nucl. Phys. A241, 386 (1975).

[42]M. H. Johnson and E. Teller, Phys. Rev. 93, 357 (1954); D. H. Wilkinson, in *Proceedings of the Rutherford Jubilee International Conference, Manchester 1961,* edited by J. B. Birks (Heywood and Company, Ltd., London, 1962), p. 339.

[43]A. Abashian, R. Cool, and J. W. Cronin, Phys. Rev. 104, 855 (1956).

[44]H. A. Bethe and L. R. B. Elton, Phys. Rev. Lett. 20, 745 (1968).

[45]R. Hofstadter, G. K. Nöldeke, K. J. van Oostrum, L. R. Suelzle, M. R. Yearian, B. C. Clark, R. Herman, and D. G. Ravenhall, Phys. Rev. Lett. 15, 758 (1965); K. J. van Oostrum, R. Hofstadter, G. K. Nöldeke, M. R. Yearian, B. C. Clark, R. Herman, and D. G. Ravenhall, Phys. Rev. Lett. 16, 528 (1966).

[46]R. D. Ehrlich, D. Fryberger, D. A. Jensen, C. Nissim-Sabat, R. J. Powers, V. L. Telegdi, and C. K. Hargrove, Phys. Rev. Lett. 18, 959 (1967); R. D. Ehrlich, Phys. Rev. 173, 1088 (1968).

[47]Y. N. Kim, *Mesic Atoms and Nuclear Structure* (North-Holland, Amsterdam, 1971).

[48]G. W. Greenlees, G. J. Pyle, and Y. C. Tang, Phys. Rev. 171, 1115 (1968); G. W. Greenlees, V. Hnizdo, O. Karban, J. Lowe, and W. Makofske, Phys. Rev. C 2, 1063 (1970); V. Hnizdo, O. Karban, J. Lowe, G. W. Greenlees, and W. Makofske, *ibid.* 3, 1560 (1971).

[49]B. Tatischeff, I. Brissaud, and L. Bimbot, Phys. Rev. C 5, 234 (1972).

[50]S. L. Tabor, B. A. Watson, and S. S. Hanna, Phys. Rev. C 11, 198 (1975); M. C. Bertin, S. L. Tabor, B. A. Watson, Y. Eisen, and G. Goldring, Nucl. Phys. A167, 216 (1971).

[51]H. A. Bethe and P. J. Siemens, Phys. Lett. 27B, 549 (1968); J. A. Nolen, Jr., and J. P. Schiffer, *ibid.* 29B, 396 (1969); J. P. Schiffer, J. A. Nolen, Jr., and N. Williams, *ibid.* 29B, 399 (1969); N. Auerbach, J. Hüfner, A. K. Kerman, and C. M. Shakin, Phys. Rev. Lett. 23, 484 (1969).

[52]G. D. Alkhazov, S. L. Belostotsky, O. A. Domchenkov, Yu. V. Dotsenko, N. P. Kuropatkin, M. A. Schuvaev, and A. A. Vorobyov, Phys. Lett. 57B, 47 (1975).

[53]E. Rost and G. W. Edwards, Phys. Lett. 37B, 247 (1971); G. Durand and J. Gillespie, *ibid.* 56B, 263 (1975).

[54]C. J. Batty and E. Friedman, Nucl. Phys. A179, 701 (1972).

[55]W. Hirt, Nucl. Phys. B9, 447 (1969).

[56]H. Alvensleben, U. Becker, W. K. Bertram, M. Chen, K. J. Cohen, T. M. Knasel, R. Marshall, D. J. Quinn, M. Rohde, G. H. Sanders, H. Schubel, and S. C. C. Ting, Phys. Rev. Lett. 24, 792 (1970).

[57]E. H. Auerbach, H. M. Qureshi, and M. M. Sternheim, Phys. Rev. Lett. 21, 162 (1968).

[58]B. W. Allardyce, C. J. Batty, D. J. Baugh, E. Friedman, G. Heymann, J. L. Weil, M. E. Cage, G. J. Pyle, G. T. A. Squier, A. S. Clough, J. Cox, D. F. Jackson, S. Murugesu, and V. Rajaratnam, Phys. Lett. 41B, 577 (1972).

[59]D. H. Davis, S. P. Lovell, M. Csejthey-Barth, J. Sacton, G. Schorochoff, and M. O'Reilly, Nucl. Phys. B1, 434 (1967); E. H. S. Burhop, *ibid.* B1, 438 (1967).

[60]E. H. S. Burhop, D. H. Davis, J. Sacton, and G. Schorochoff, Nucl. Phys. A132, 625 (1969).

[61]W. M. Bugg, G. T. Condo, E. L. Hart, H. O. Cohn, and R. D. McCulloch, Phys. Rev. Lett. 31, 475 (1973).

[62]H. A. Bethe and P. J. Siemens, Nucl. Phys. B21, 589 (1970).

[63]Study of the two-neutron form factor as a function of Z or the two-proton form factor as a function of N would involve an investigation of the effective proton-neutron residual interaction in the nucleus.